

# Global Tropospheric Aerosols

Y. Iwasaka

(Nagoya University)

# Global Tropospheric Aerosols

:Long-range Transport and Its Effect on Global Environment

Yasunobu Iwasaka

Solar Terrestrial Environment Laboratory, Nagoya University

Chikusa-ku, Nagoya 464

## Abstract

The lidar measurements made at Nagoya, Japan show the possibility that asian continent soil particles disturb the mid-troposphere over Japan.

Number-size distribution function made with air-borne instruments over Japan in 1991-1994 frequently shows peak in the range of diameter;  $D \geq 1 \mu\text{m}$  in the free troposphere. Those are confirmed by the lidar measurements. On the basis of backward trajectory analysis of the air mass containing those particles, soil particles originated in Asian continent affect on the features found in the size distributions, and environment through global diffusion of particulate matter originated in the Asian continent.

## 1. Introduction

In every spring, Asian dust particles are frequently transported to Japan by westerly prevailing wind. Particularly, heavy dust storms apparently observed near the ground in Japan are familiarly called 'Kosa' in Japanese. Those soil particles are found also over the North Pacific Ocean as described in studies by Duce et al. (1980), Shaw (1980), Darzi and Winchester (1982) and Uemats et al. (1983) and others. Lidar measurements made at Japan showed that many Kosa particle layers with a few kilometers frequently appeared in the free troposphere even when Kosa episode was not detected near the ground (Iwasaka et al., 1988), suggesting long range transport of soil particles in the mid troposphere. Backward trajectory analysis of air mass containing Kosa particles (Merrill et al., 1985) and numerical simulation (Kai et al., 1988) suggested the possibility that Kosa particles transported over Japan in the free troposphere without severe Kosa episode in Japan and to Pacific Ocean.

Morphological observation of the particles with an electron microscope (e.g., Okada et al., 1990) showed that irregular shape particles dominated in super micron range in the boundary atmosphere during Kosa episode. Chemical analysis of atmospheric particulate matter collected during the period of dust storm episode (e.g., Gao et al., 1992; Betzer et al., 1988) indicated sudden increase in concentration of metals such as Ca, Al, and so on which were thought to be major composition of soil particles. X-ray analysis of individual particles collected during Kosa episode (Okada et al., 1990) also showed increase in content of those metals. Iwasaka et al. (1988) found the airborne particles which surface was coated with thin solution film containing SO<sub>4</sub><sup>2-</sup> from the particle collection in the free atmosphere over Japan.

Radiative effect of the dust storm particles (e.g., Arao and Ishizaka, 1986; Asano and Siobara, 1989, Hayasaka et al., 1992; Tanaka et al., 1990) was studied and suggested that load of Kosa particles in the troposphere over Japan disturbed largely radiative balance.

In previous observations, there is limited information concerning with size, concentration and chemical composition of free atmospheric aerosols including Kosa over Japan.

Airborne measurements on the size distribution patterns of free

tropospheric aerosols were made in the spring of 1991-1994 to understand behavior of particulate matter over Japan. Westerly prevailing winds seem to characterize nature of atmospheric particles over the east Asia and the western Pacific region since the wind frequently carries particulate matter originated in the continent over the ocean and sometimes such particle is expected to be major in those regions (e.g., Duce et al., 1983).

Main purpose of this paper is to provide particle size distribution patterns measured over Japan and to discuss the effect of soil particles originated in Asian continent on the size distributions of the free tropospheric particles over Japan.

## 2. Free Tropospheric Aerosol Concentration Measured with a Lidar in Spring

Aerosol content was observed at Nagoya in 1994 with the lidar which has the characteristics described briefly in Table 1. Scattering ratio of particulate matter is defined by

$$\text{Scattering Ratio} = [\beta_1 + \beta_2] / \beta_1,$$

where  $\beta_1$  and  $\beta_2$  are backscattering coefficient of air molecules and atmospheric aerosols. The mixing ratio of particulate matter observed with a lidar, therefore, can be derived from

$$\begin{aligned} \text{Mixing Ratio} &= \beta_2 / \beta_1 \\ &= \text{Scattering ratio} - 1. \end{aligned}$$

Scattering ratio of tropospheric aerosols measured in spring (April and May, 1994) is compared with that in summer (July and August, 1994). In spring highly concentrated particle layer with a few kilometers thickness are frequently observed but not in summer.

Depolarization ratio defined as follow is used to detect nonspherical particles,

$$\text{Depolarization Ratio} = \beta_{\perp} / \beta_{\parallel}$$



where  $\beta$  is total backscattering coefficient including  $\beta_1$  and  $\beta_2$ , and suffix  $\perp$  and  $\parallel$  mean cross and parallel plane component of backscatter light to the plane of emitted laser light, respectively. The depolarization ratio defined above can be recognized as depolarization ratio of particulate matter here since backscatter light intensity from particulate matter is extremely larger than that from air molecules in the troposphere. Depolarization ratio of aerosols becomes 0 when light is scattered by spherical particles, and the values increase for scattering of nonspherical particles.

Depolarization ratio suggests that the particles in spring time frequently show large nonsphericity.

### 3. Discussion and Summary

From microscopic measurements of particles collected at 4.42 km, irregular shape particles, possibly soil particles, with diameter  $\geq 10 \mu\text{m}$  were frequently identified. Discrepancy between our results and those obtained in the marine free atmosphere over south west Pacific is caused mainly by soil particles transported from Asia to Japan.

Backward trajectory analysis of air mass corresponding to the height of the aerosol layer detected by the lidar was made on the surface of isopotential temperature. The analysis indicates that most of the air mass came from Asia continent with in several days, as shown in the samples of analysed trajectories.

The trajectory suggests that sometimes air mass noticeably moves up and down during its travel. The large upward motion of air mass can compensate descending movement of extremely large size particles contained in the air mass and consequently make it possible for the large particles larger than several microns to travel long distance.

Some investigations suggested one possibility that soil particles frequently transported from the Asian continent in the free troposphere over Japan with lidar observation (Iwasaka et al., 1988) and airborne polar nephelometer (Hayasaka et al., 1990).

The measurements made over Goto islands (Southern area of Japan) on Mar. 8, 1993 is a good example showing large enhancement of Kosa particles in the free troposphere, and disturbance of Kosa at the lower altitude is apparently small. In the measurements of May 12, 1993 and

Apr. 26, 1994 typical single mode spectra with mode diameter of about 1.5  $\mu\text{m}$  was observed at 4.42 km level, but bimodal function was identified at 2.29 km level suggesting disturbance of the boundary layer. Such stratified layer structure suggested that aerosol concentration above the mixed boundary layer frequently affected by soil particles transported from the Asian continent.

Radiative forcing of atmospheric particulate matter becomes great concern and long-term monitoring of atmospheric aerosols over the asian continent-pacific region with a lidar should make important contribution to study on global climate and environment changes.

Fig. 2. Time-height cross section of depolarization ratio observed by the Raman lidar. Panel A is observation on April 11, panel B on August 8, 1994, in Nagoya, Japan.



Fig. 1. Time-height cross section of scattering ratio observed by the Raman lidar at wavelength 1064 nm. Panel A is observation on April 11, panel B on August 8, 1994, in Nagoya, Japan.

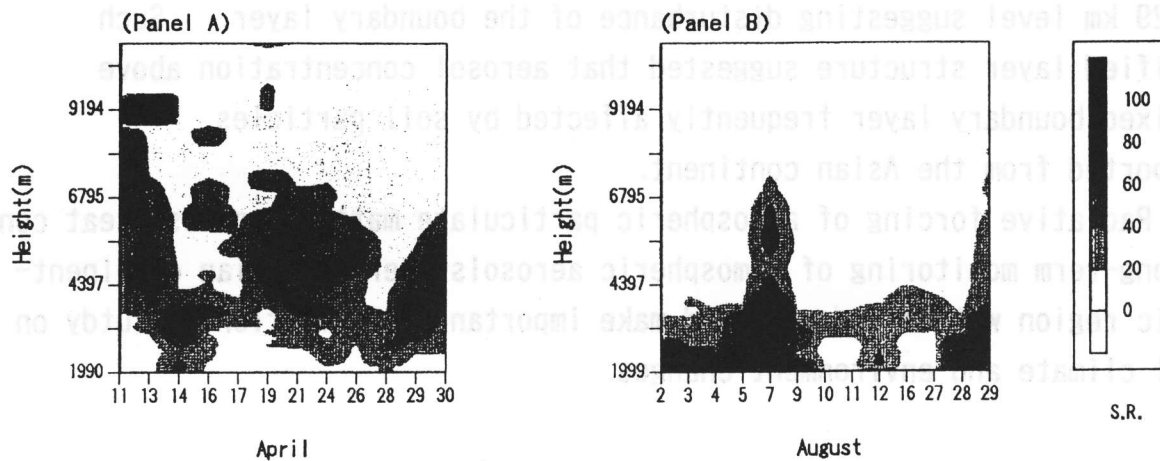


Fig. 2. Time-height cross section of depolarization ratio observed by the Raman lidar. Panel A is observation on April, panel B on August 1994, in Nagoya, Japan.

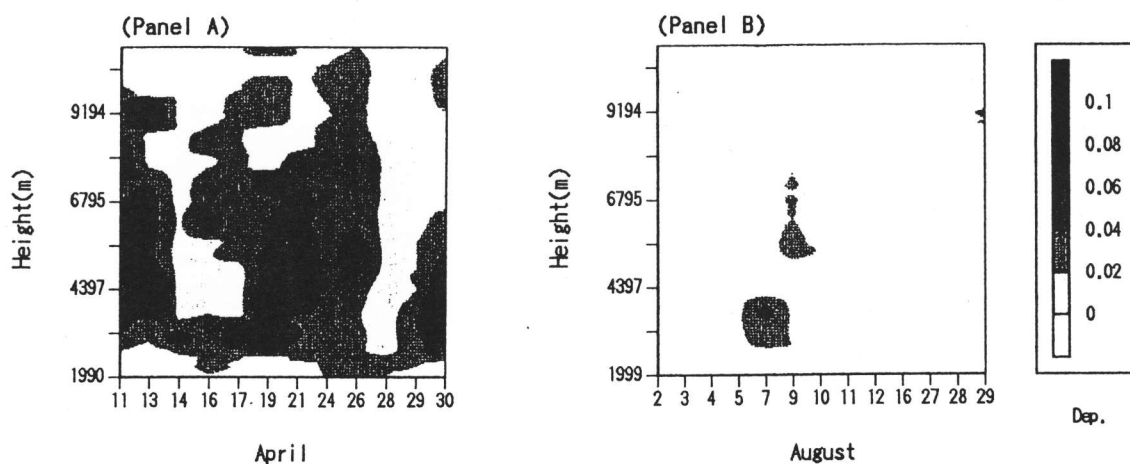


Fig. 1. Time-height cross section of scattering ratio, observed by the Raman lidar at wavelength 1064 nm. Panel A is observation on April, panel B on August 1994, in Nagoya, Japan.

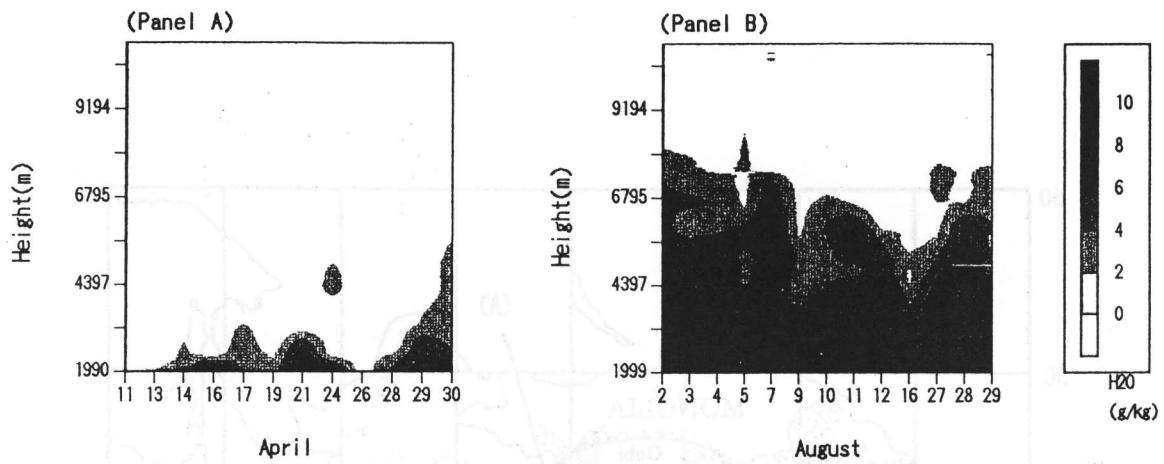


Fig. 3. Time-height cross section of water vapor mixing ratio(g/kg) observed by the Raman lidar. Panel A is observation on April, panel B on August 1994, in Nagoya, Japan.

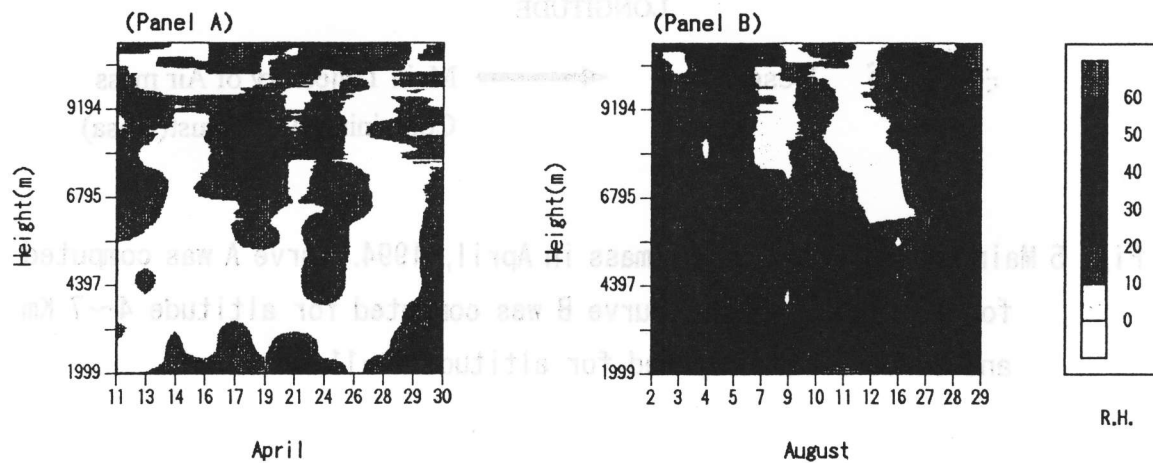


Fig. 4. Time-height cross section of relative humidity(%) observed by the Raman lidar. Panel A is observation on April, panel B on August 1994, in Nagoya, Japan.

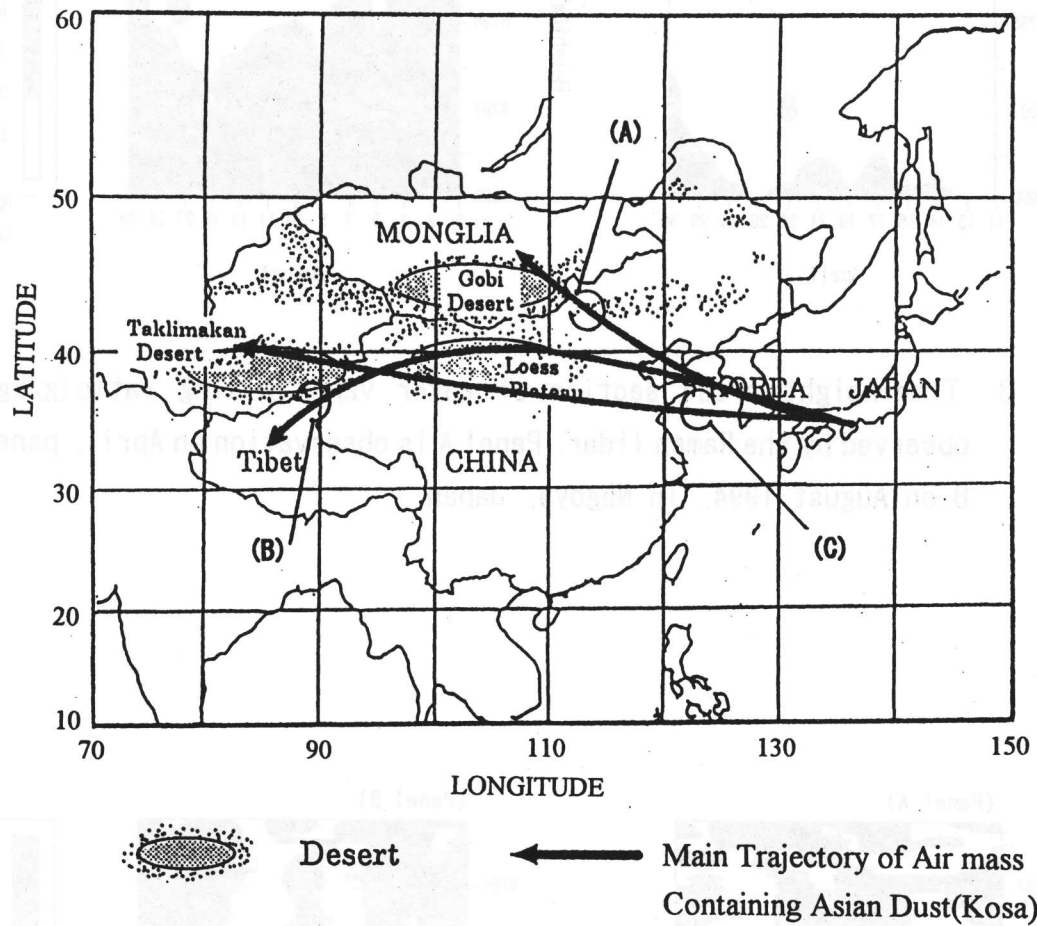


Fig. 5 Main trajectories of air mass in April, 1994. Curve A was computed for altitude 2~4 Km, curve B was computed for altitude 4~7 Km and curve C was computed for altitude 7~11 Km.



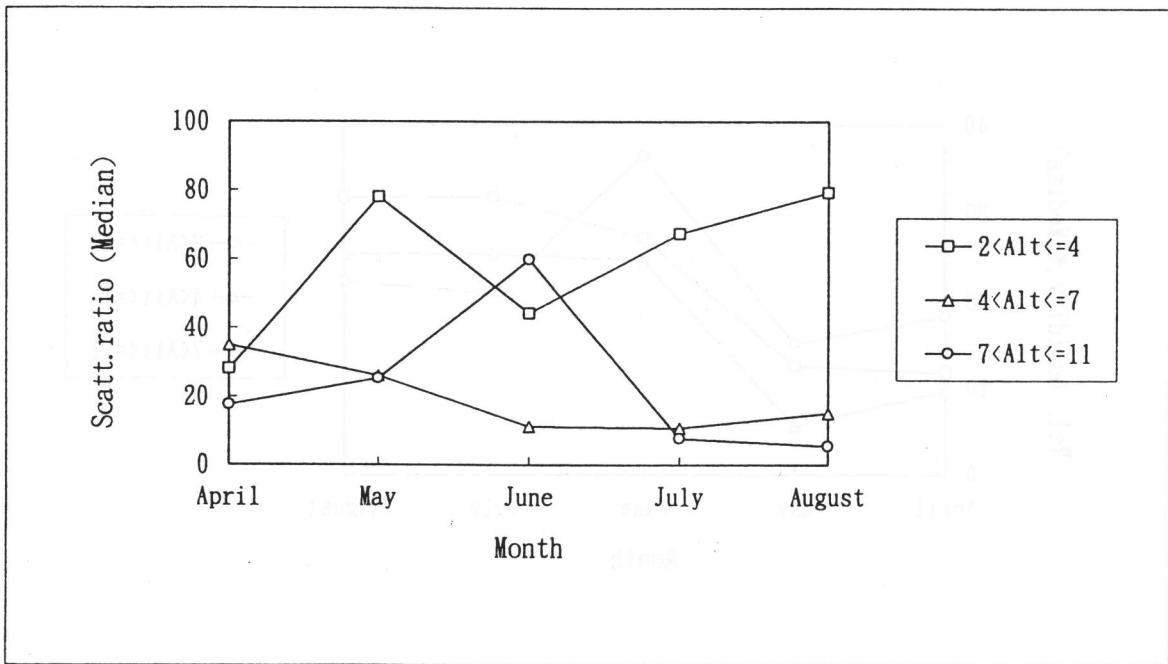


Fig. 6 The median of scattering ratios measured monthly at 1064 nm wavelength at height range of 2~4, 4~7, and 7~11 Km in April-August 1994.

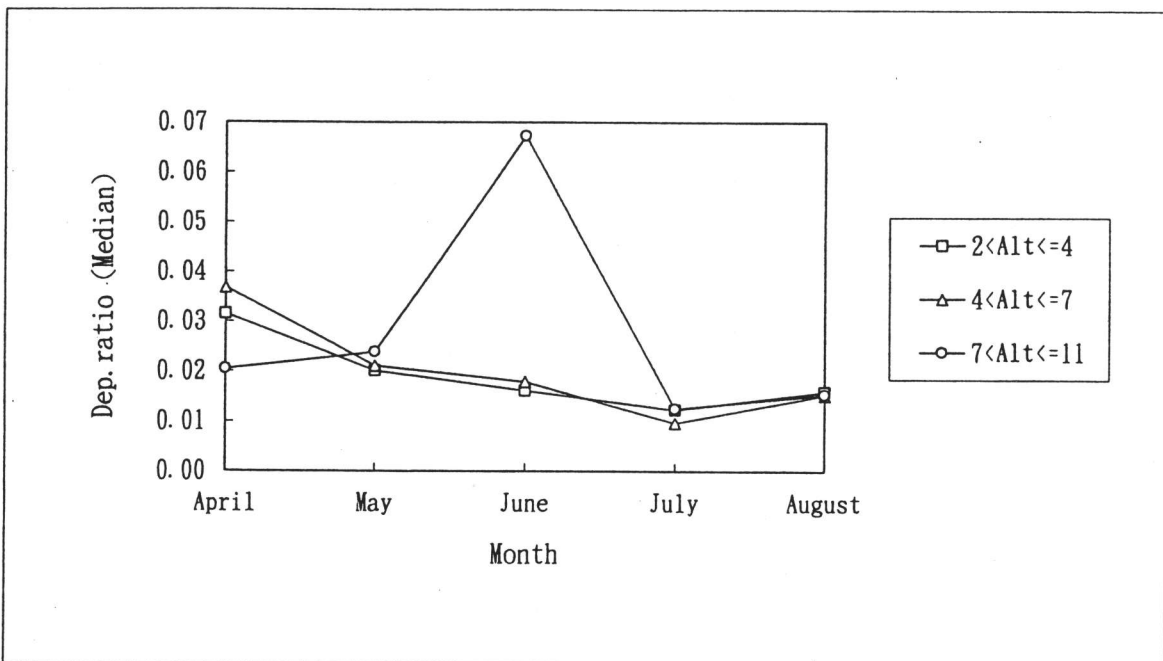


Fig. 7 The median of depolarization ratios measured monthly at height range of 2~4, 4~7, and 7~11 Km in April-August 1994.

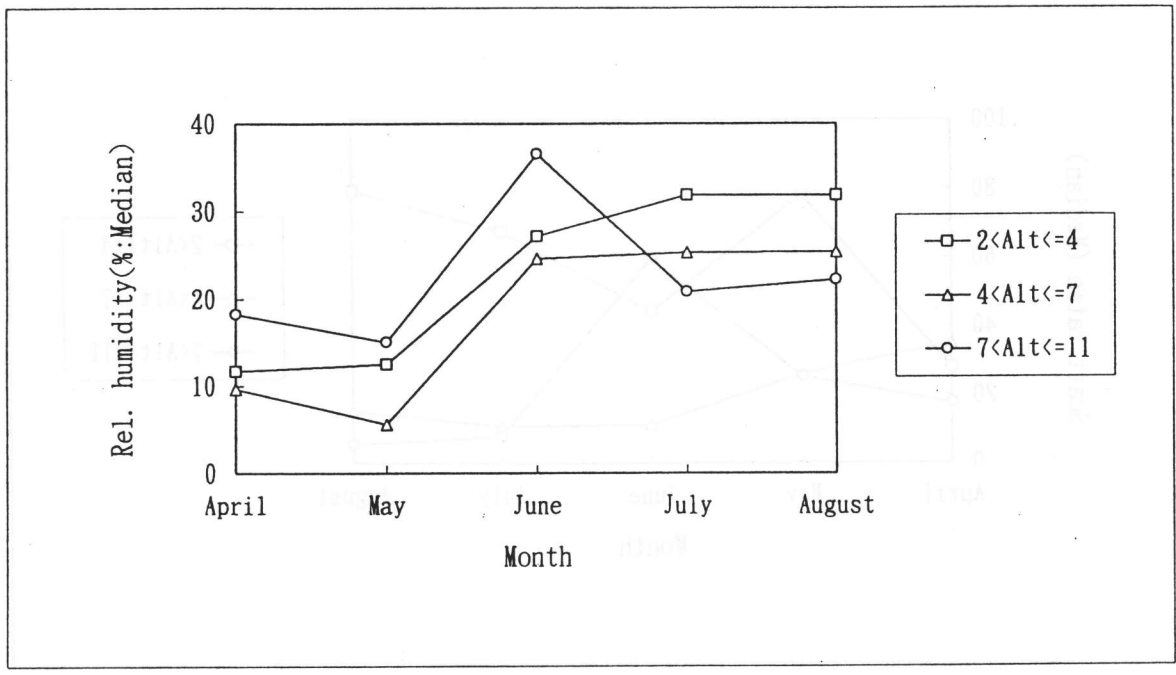


Fig. 8 The median of relative humidity measured monthly at height range of 2~4, 4~7, and 7~11 Km in April-August 1994.



The median of relative humidity measured monthly at height range of 2~4, 4~7, and 7~11 km in April-August 1994.

---

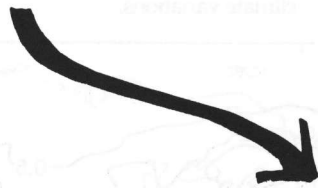
# Global Tropospheric Aerosol

Y. IWASAKA

岩坂 泰彦

---

- Balloon Measurements  
at Beijing, China  
中国気球観測
- Lidar Measurements at NAGOYA  
名古屋でのライダー観測



Importance of Monitoring of  
Tropospheric Aerosols  
on the Global Scale

特々！

## 8. What else influences radiative forcing?

### 8.1 SOLAR VARIABILITY

We know that total solar irradiance varies with an 11-year cycle. Space-borne satellite measurements available since 1978 show that over the most recent sunspot cycle the changes in solar irradiance were equivalent to a radiative forcing of about  $0.2 \text{ W m}^{-2}$ . This may initially seem significant, given that it is an appreciable fraction of the forcing due to greenhouse gases over the same period. However, these changes in solar irradiance are cyclical in nature and it is believed that, due to the thermal inertia in the climate system, only a small amount of the possible temperature change resulting from such transient changes in irradiance is realised. In contrast, the changes in greenhouse gases represent a sustained and cumulative effect over many decades.

Recent satellite observations show a relationship between total solar irradiance and other indicators of solar activity which allows a tentative reconstruction of past total solar irradiance. Although there is considerable uncertainty in estimating solar irradiance before direct measurements began, changes in solar irradiance since 1850 may have contributed a natural radiative forcing of around  $0.3 \text{ W m}^{-2}$  (Figure 3). Future forcing due to changes in solar irradiance could be negative or positive.

### 8.2 VOLCANIC ACTIVITY

Volcanic eruptions can act to increase the amount of aerosol particles in the stratosphere. The dominant radiative effect is an increase in scattering of solar radi-

ation which reduces the net radiation available to the surface/troposphere, thereby leading to cooling. Volcanoes have the potential to produce large radiative forcing, but the events are transitory.

The eruption of Mt. Pinatubo in the Philippines in June 1991 stands out from a climatic point of view as probably the most important eruption this century. The largest forcing is calculated to have been about  $-4 \text{ W m}^{-2}$  around one year after the eruption. This decayed to around  $-1 \text{ W m}^{-2}$  after 2 years. Thus, the radiative forcing resulting from Mt. Pinatubo for the first 2 years after the eruption was comparable, but of opposite sign, to the greenhouse gas forcing this century ( $+2.1$  to  $+2.8 \text{ W m}^{-2}$ ). A cooling of global surface temperature observed following the eruption reached a maximum of  $0.3$  to  $0.5 \text{ }^\circ\text{C}$  during 1992. Simulation of the climatic effects of Mt. Pinatubo aerosols using general circulation models (GCMs) have produced results in good agreement with observations, with a maximum cooling of  $0.4$  to  $0.6 \text{ }^\circ\text{C}$ . Such simulations increase confidence in the ability of GCMs to respond in a realistic way to transient, planetary-scale radiative forcings of large magnitude.

Clearly, individual volcanic eruptions can produce large radiative forcing effects, but these effects are transitory. An important issue here is whether changes in greenhouse gases and aerosols due to human activity are significant compared with natural factors. A key question is therefore whether there has been any trend in volcanic activity over the period since industrialisation; this is unlikely. However, variations in the occurrence of climatically significant eruptions may be a factor in explaining some interannual and interdecadal climate variations.

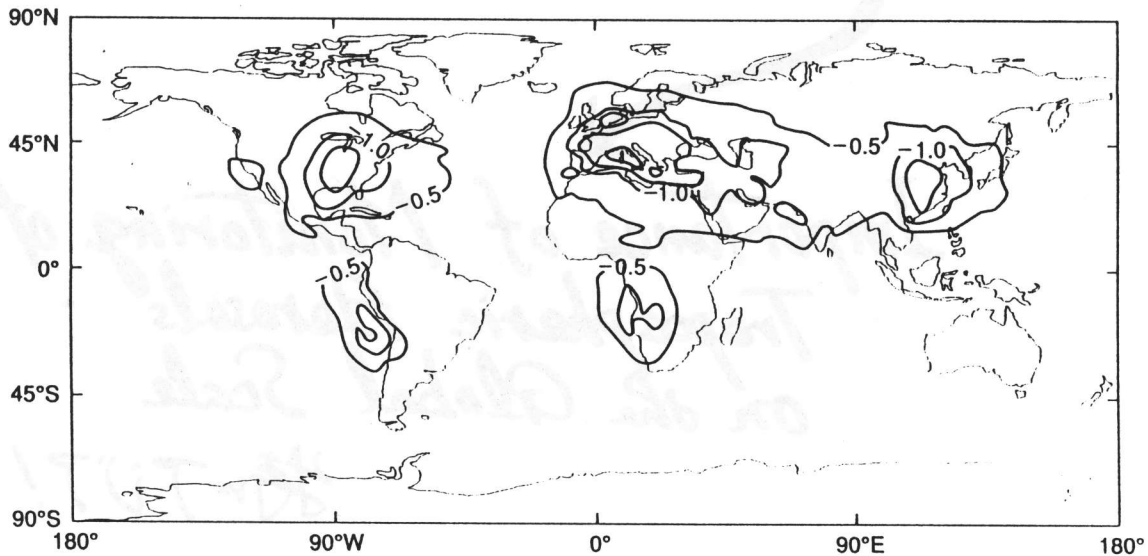
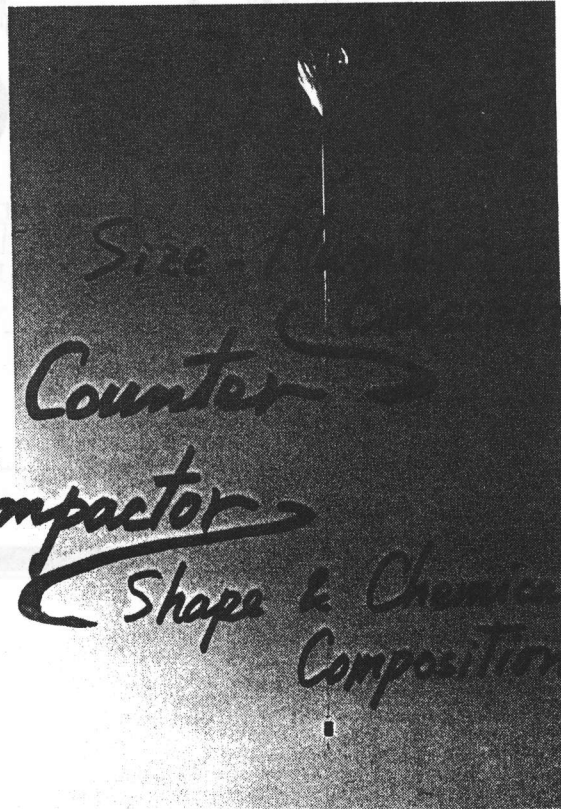
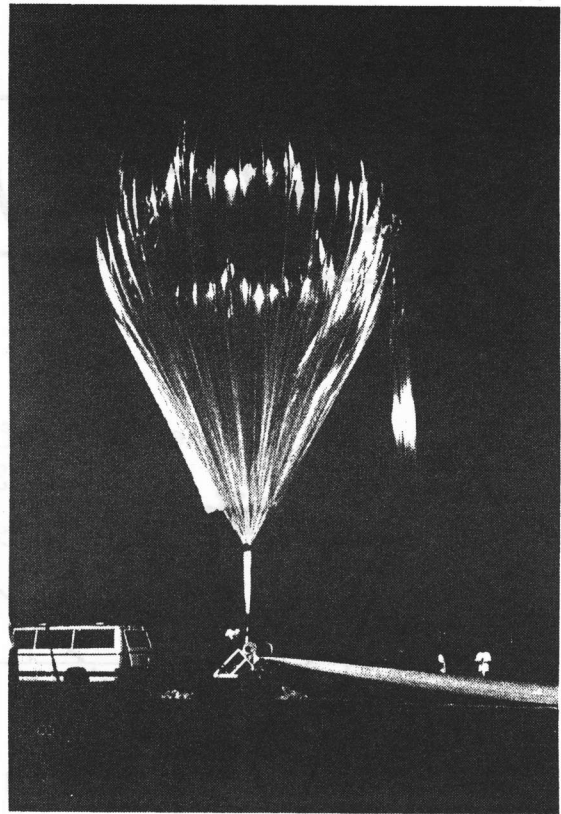


Figure 12. Modelled geographic distribution of annual mean direct radiative forcing ( $\text{W m}^{-2}$ ) from anthropogenic sulphate aerosols in the troposphere. The negative radiative forcing is largest over or close to regions of industrial activity.





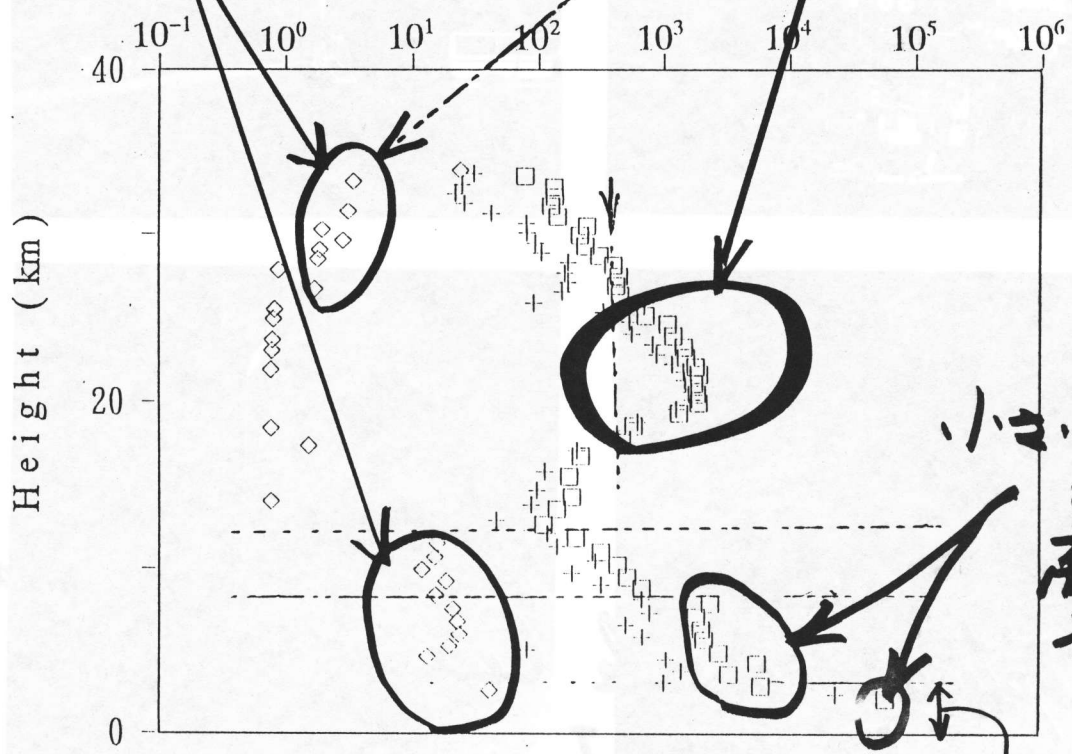
# 光散乱方式パーティクルカウンター

## 成層圏エアロゾル

大きい粒子の分布

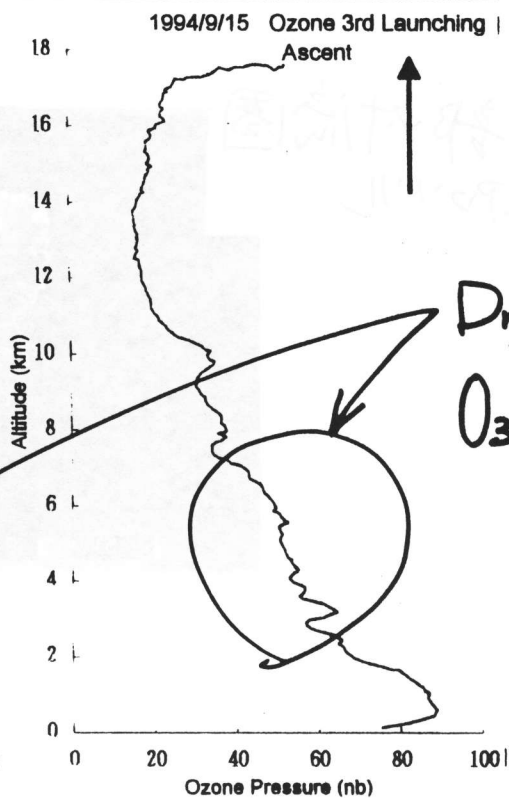
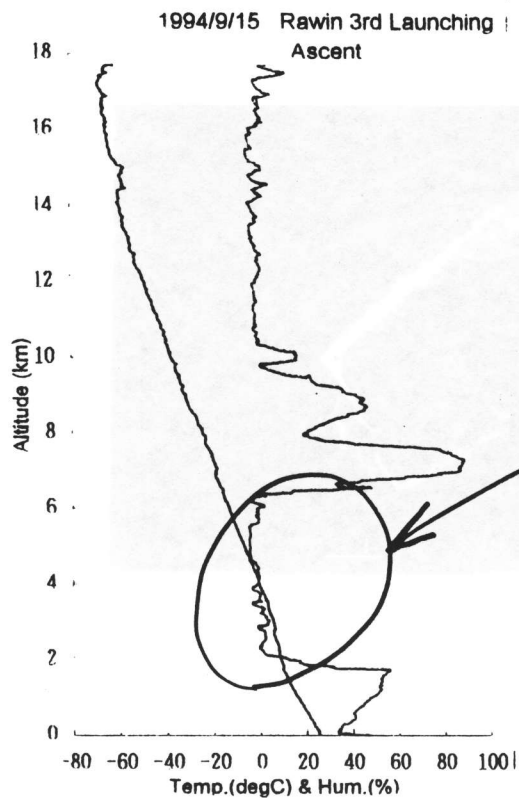
Aerosol Profile over Xianghe  
1993. 8. 22  
Particle Concentration (/liter)

Pinatubo effect

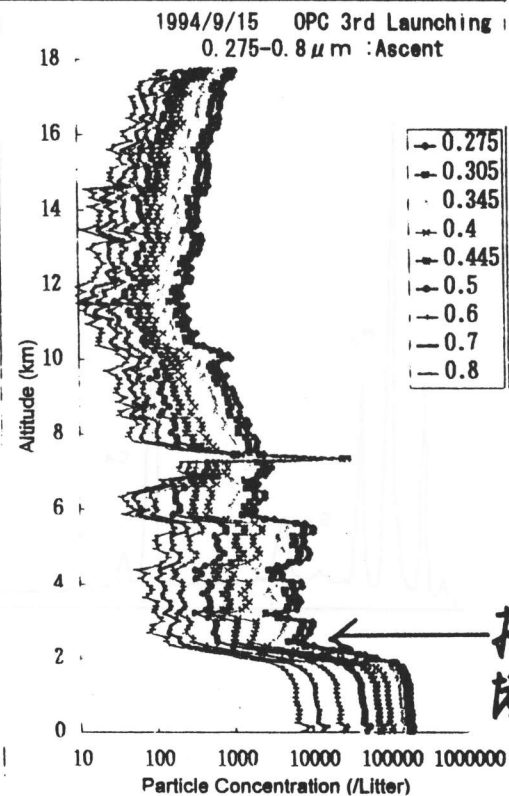
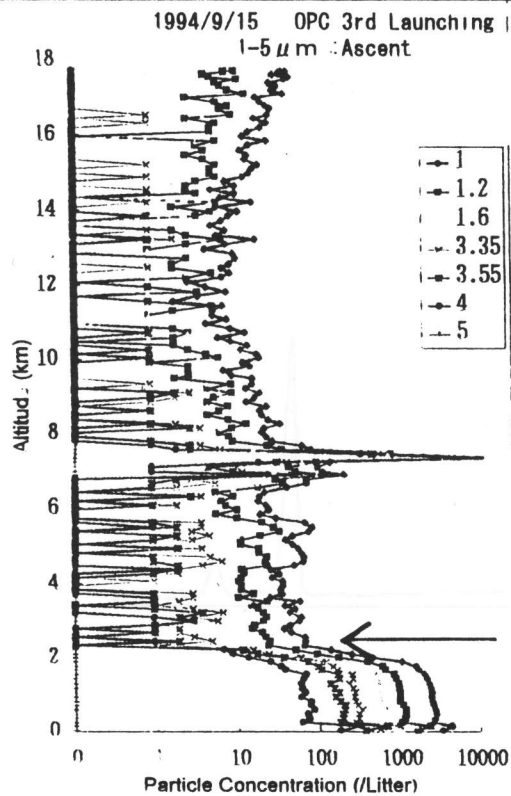


小さい粒子高濃度

接地境界層



Dry  
O<sub>3</sub> 高濃度



接地  
境界層

中部対流圏  
エロソール



Fig.3-5 Type1-a.;非球形型(Coarse)ーフラット (写真) とそのEDX分析結果 (下)  
(8/25/94 : 8.5~9.5 km) 元素記号のついていないピークはバックグラウンド

上部対流圏  
エアゾール

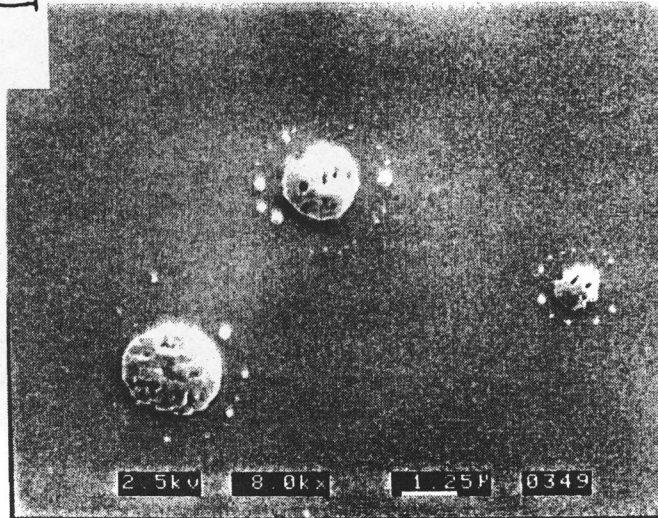


(写真) 上部対流圏(約12.7 km)に存在するエアゾール中の液滴 (8/25/94 ; 20.8~21.7 km)

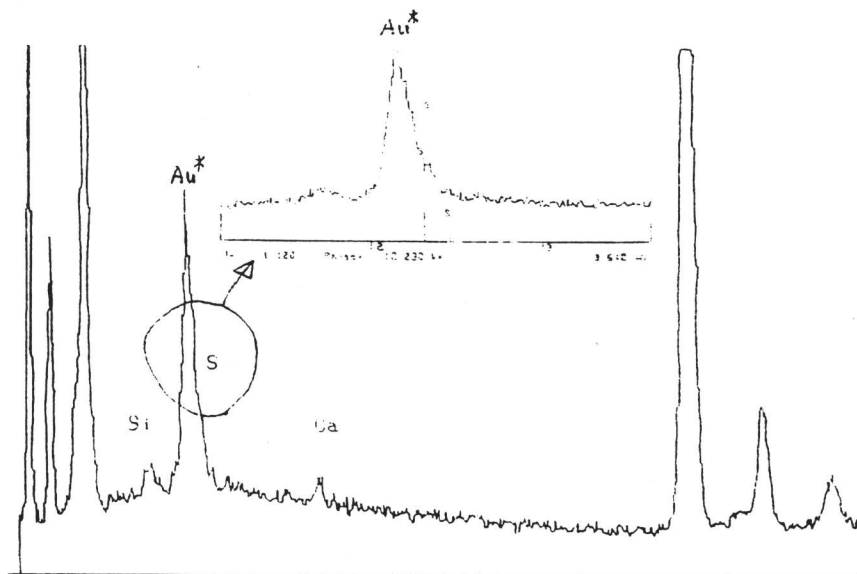


Fig.3-9 Type3:液滴(Liquid-droplet) (写真) とそのEDX分析結果 (下)  
(8/25/94 ; 12.7~11.5 km) 元素記号のついていないピーク及び Au\*  
(金蒸着のため) はバックグラウンド.

衛星構造

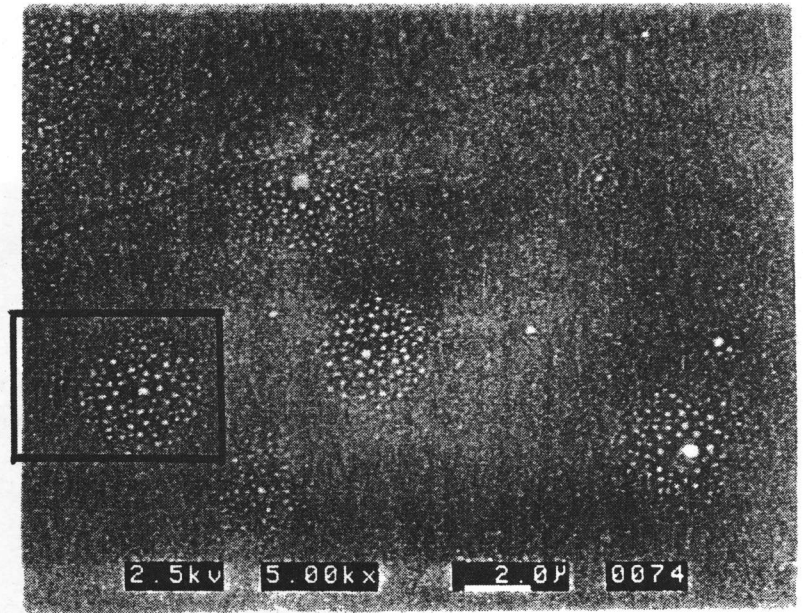
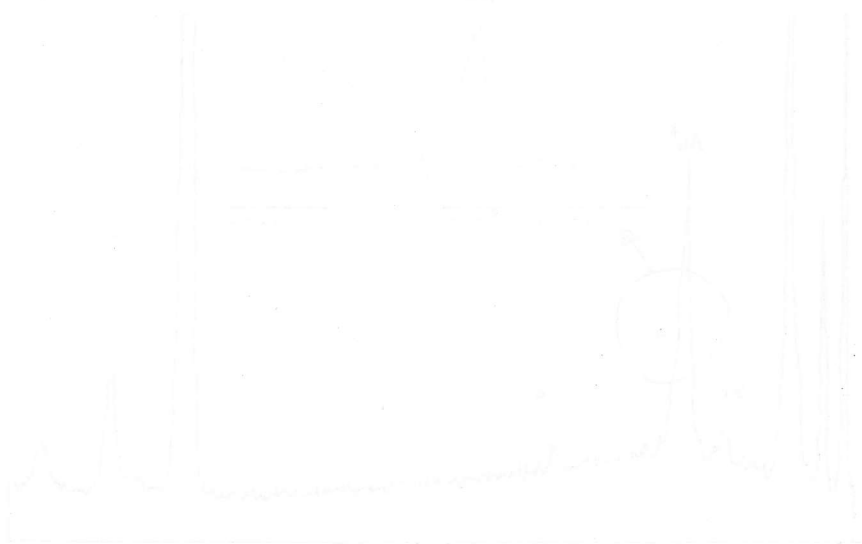


Fig.3-18 中心核のないサテライト構造を持った粒子 (写真)  
(8/22/93 ; 20.6~21.7 km)

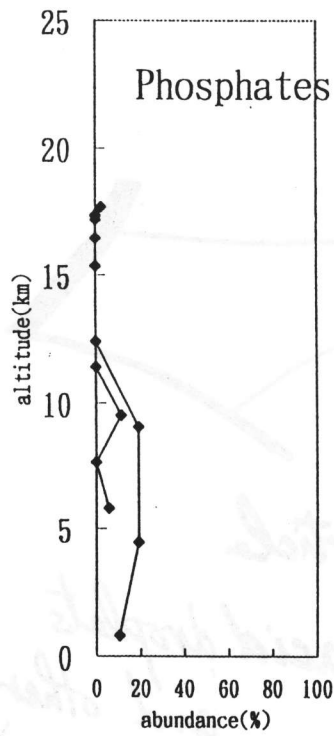
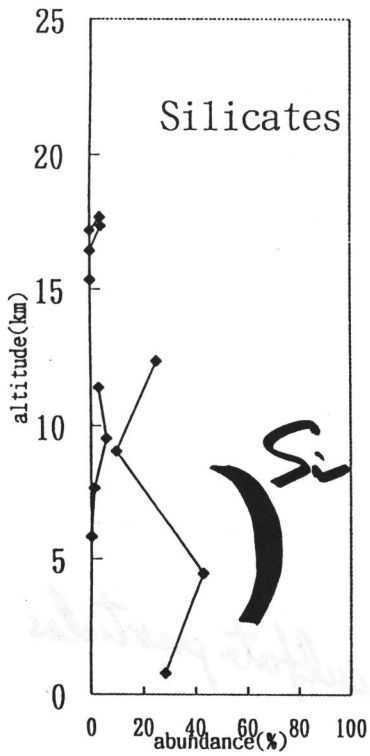


(下) 果敢図名XG Eの(子) (原) (1990-1991) (T 9-8) (1992)  
(1992) (1992) (1992) (1992) (1992) (1992) (1992) (1992) (1992) (1992)  
(1992) (1992) (1992) (1992) (1992) (1992) (1992) (1992) (1992) (1992)

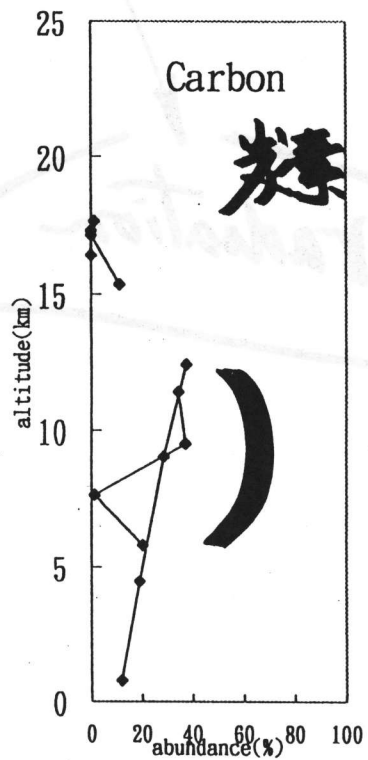
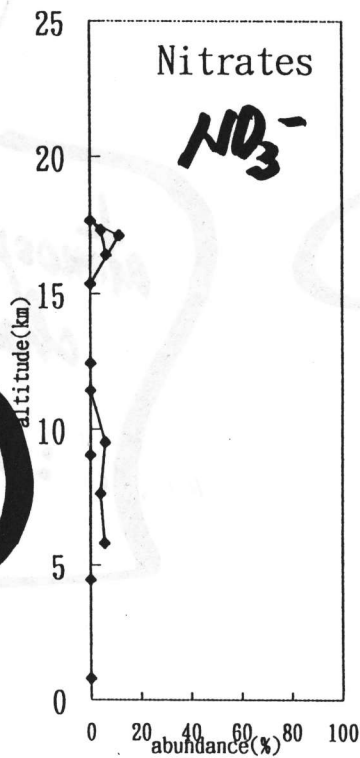
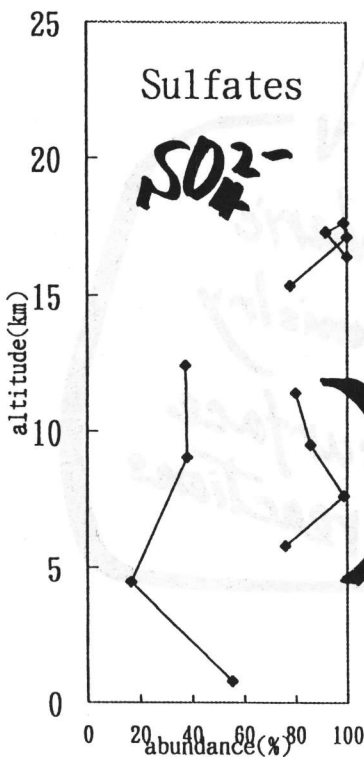


# IAMMAS

9/15 '94



### Continuum



Asian  
Continent

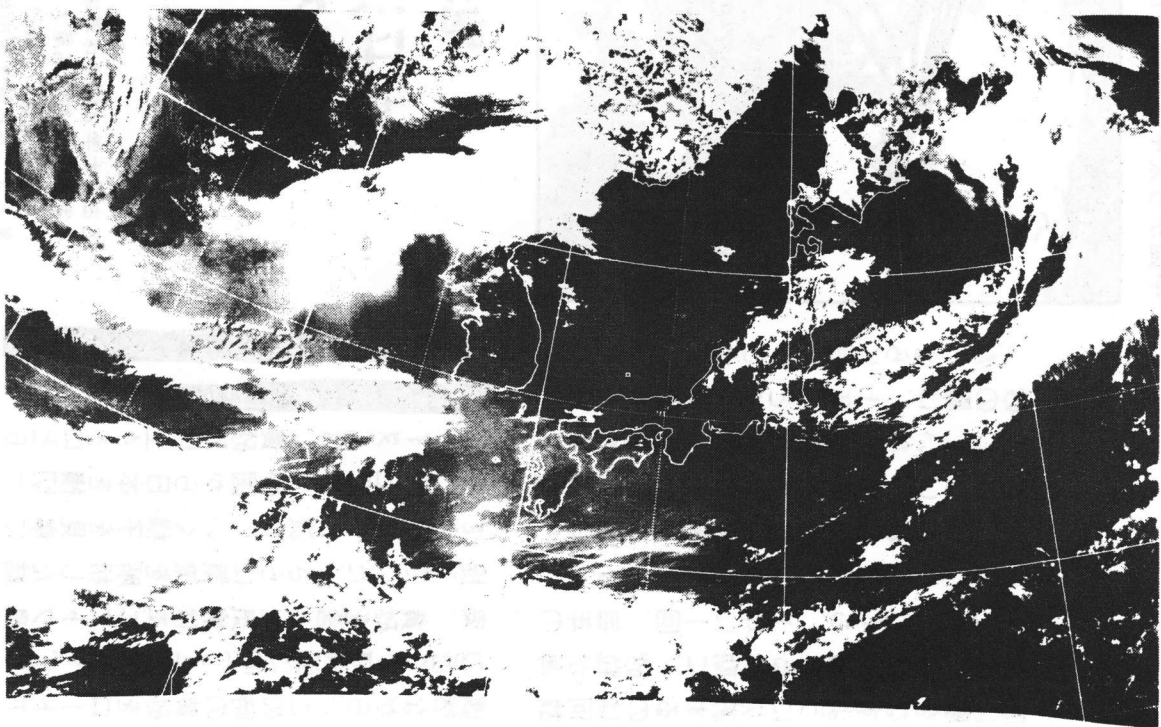
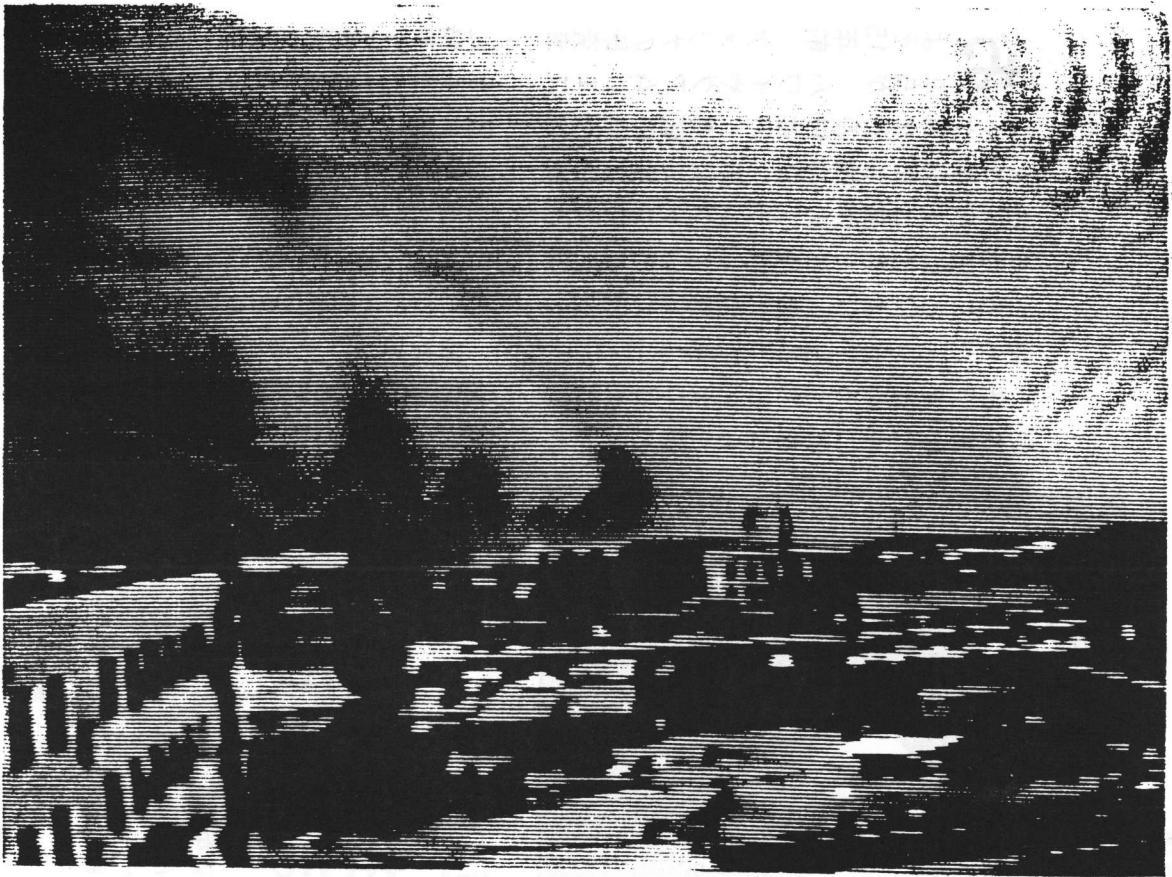
soil particle

sulfuric acid droplets  
and other sulfate particles

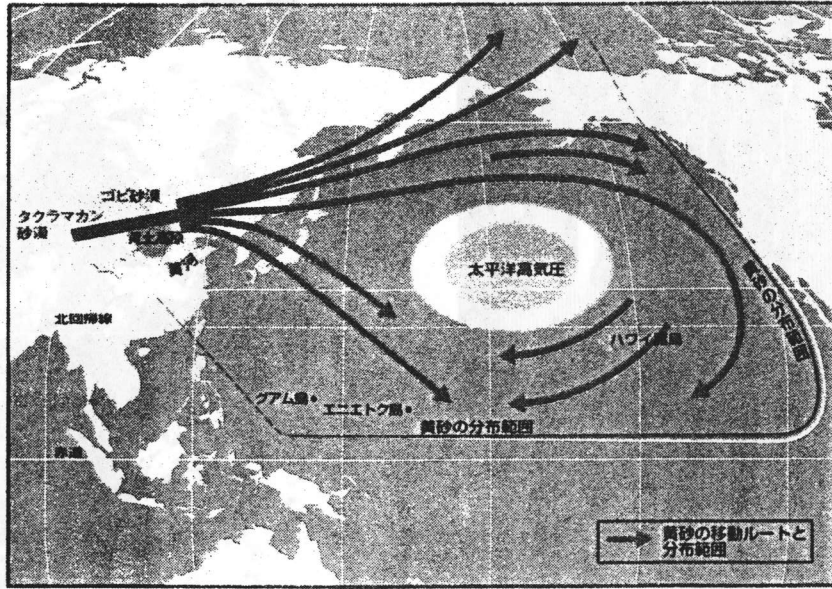
radiation

atmospheric  
chemistry

: surface  
reactions



中国から太平洋一帯へと飛来する黄砂



お よそ15年前、アメリカの研究  
 たちが、ハワイやグアム、エニ  
 エトク島などの付近の、海底の堆積物  
 を化学分析し始めた。研究の主な目的  
 は、例えば海中のプランクトンの死骸  
 が海底にどれだけ堆積しているかを調  
 べることに、海の状態の歴史を  
 明らかにしようとするのであった。  
 研究を進めるうちに、太平洋の海底  
 の沈澱物の中に砂を含んだ層が見つ

た。さらに面白いことに、それらの  
 砂の層は、1年ごとに規則正しく層を  
 成していた。海中で砂粒が生まれるは  
 ずはない。そこでアメリカの研究者た  
 ちは、これらの砂粒が大気から海洋へ  
 ともたらされたものであろうと考えた。  
 それにしても、1年に1回、毎年  
 のように春に相当する時期に、砂粒が海  
 底に層をなすように沈澱するのは何故  
 なのか。彼らはこれが、東アジアの春

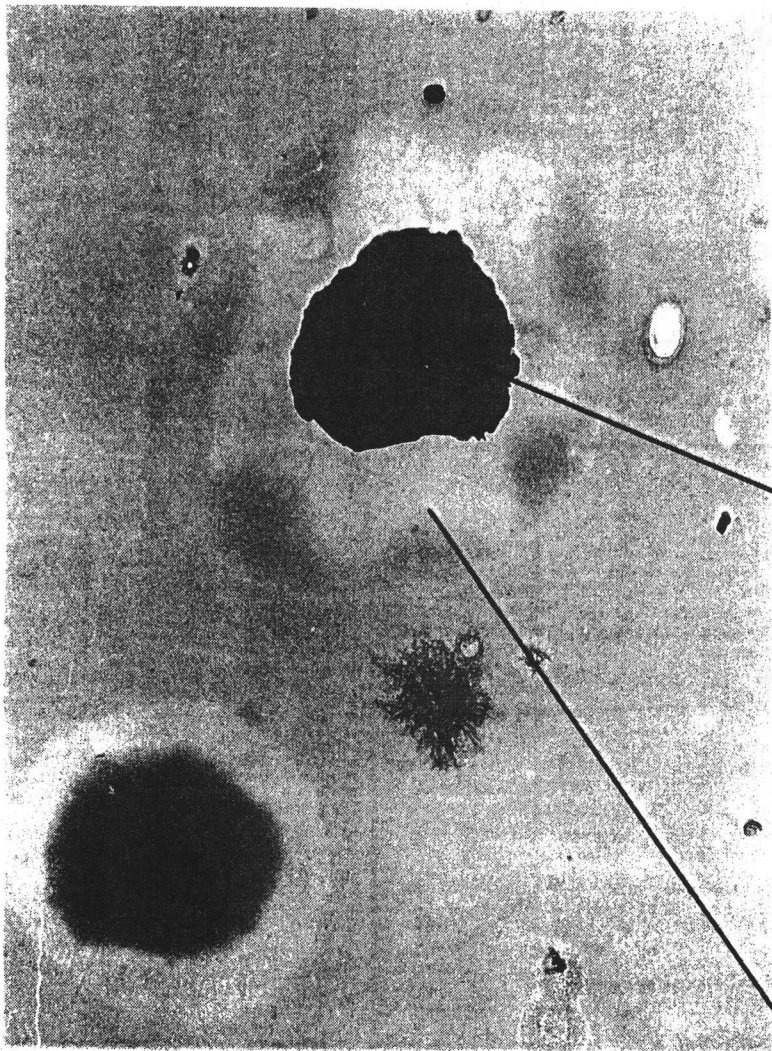
地球環境の神秘  
 太平洋の生態系に  
 影響を及ぼす黄砂

文◎岩坂泰信  
 Text by Yasunobu Iwasaka

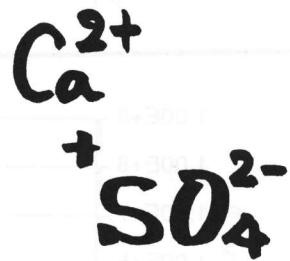
いわさか やすのぶ  
 名古屋大学太陽地球環境研究所教授 専攻分野は中層大気物理学。1941  
 年生まれ 新型の高層大気観測装置 ライダーで大気の観測を続けて  
 いる 主な著書に「黄砂」古今書院 オールホール 裳華房「環境を  
 考える」名古屋大学出版会など

に特有な「黄砂」と呼ばれる現象と関係  
 があるかも知れないと考え始めた。中  
 国大陸の砂塵嵐によって空中に巻き上  
 げられた砂粒が、西風によって日本へ  
 と流れてくる黄砂は、日本人、特に西  
 日本人のたちにとりては、春の風物詩  
 の一つとして身近なものになっている。  
 私たちは、1979年の春の黄砂を

ライダーは、黄砂が地上4キロと6  
 キロの上空を、中国から日本を横切  
 して太平洋へと流れていく様子を見事に  
 捉えていた。さらに気流を解析した結  
 果、黄砂を含んだ気塊はエニエトク島  
 の近くで海表面に向かって下降していた。  
 偶然ながら、この時の黄砂をロードア  
 イランド大学の研究チームが捕まえて



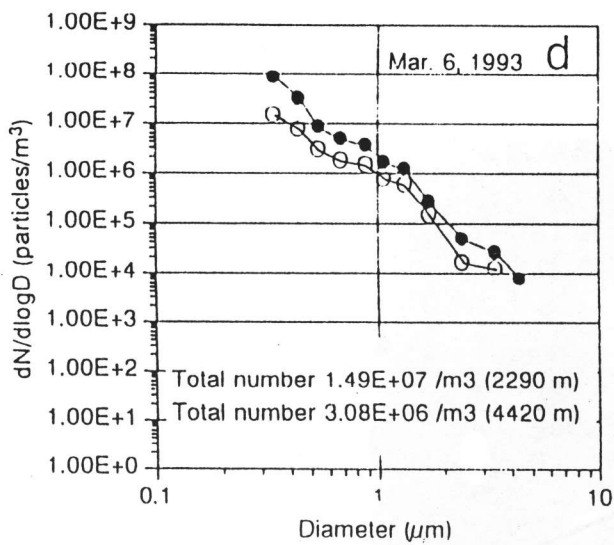
Soil



4km Over NAGOYA

Collected Soil Particles  
on Ca thin film surface

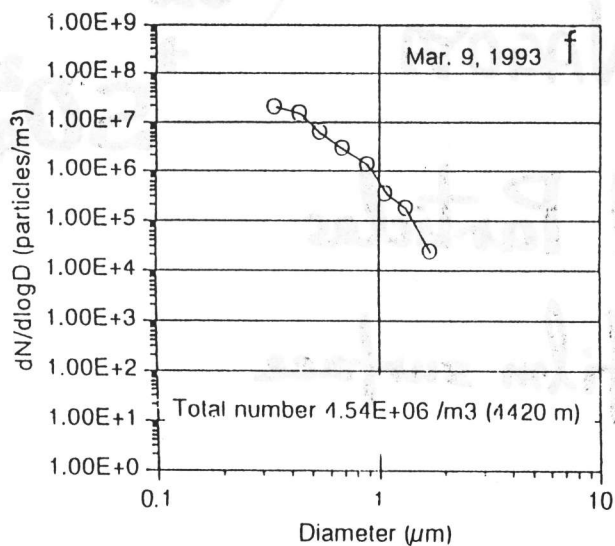
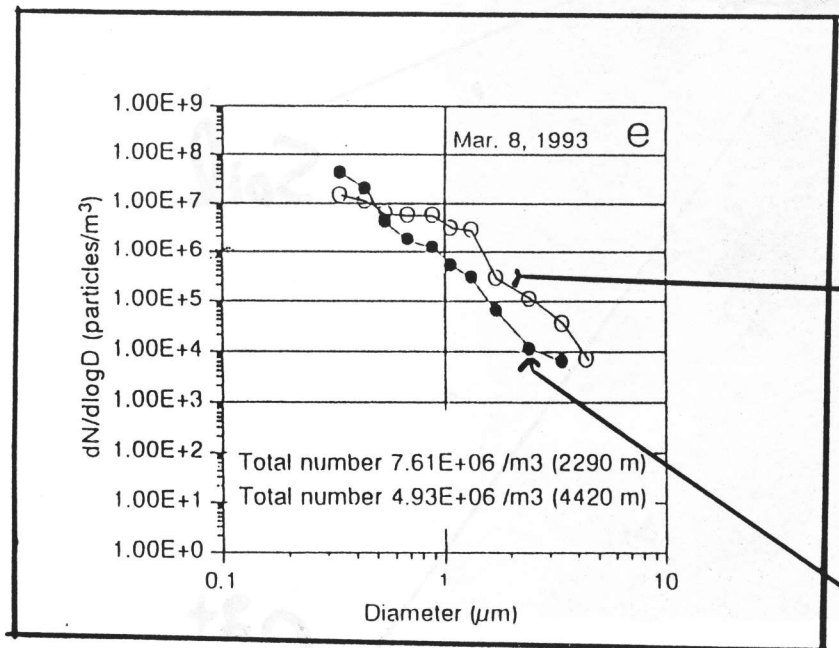




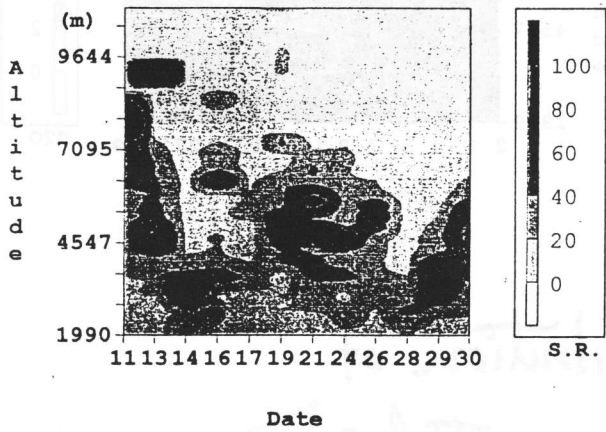
# Number - Size Distribution

over

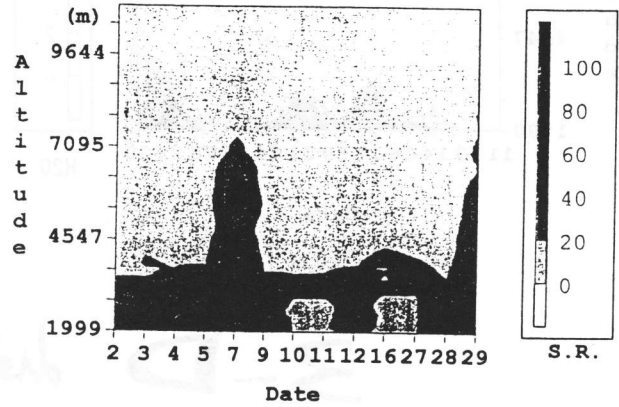
NAGOTA  
March, 1993



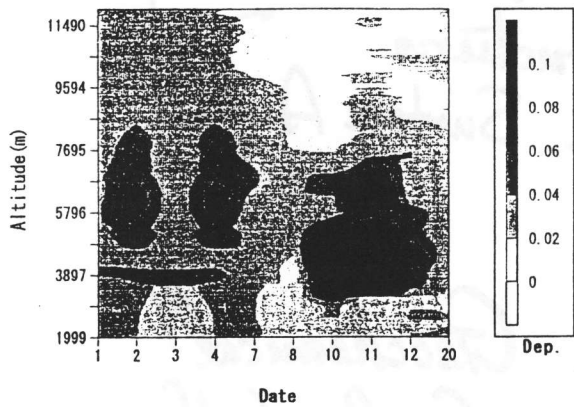
Scattering ratio (1064nm)  
April, 1994. at Nagoya



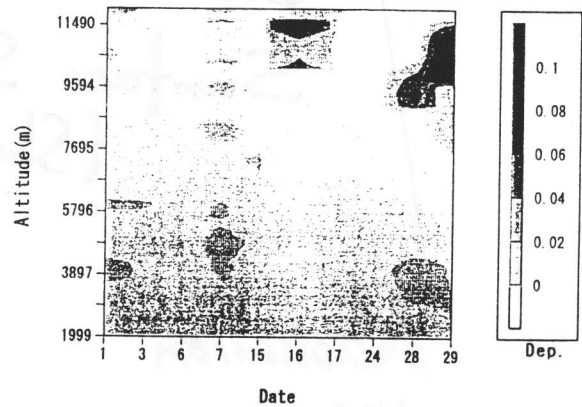
Scattering ratio (1064nm)  
at Nagoya, August, 1994.



Depolarization ratio  
at Nagoya, April, 1995.

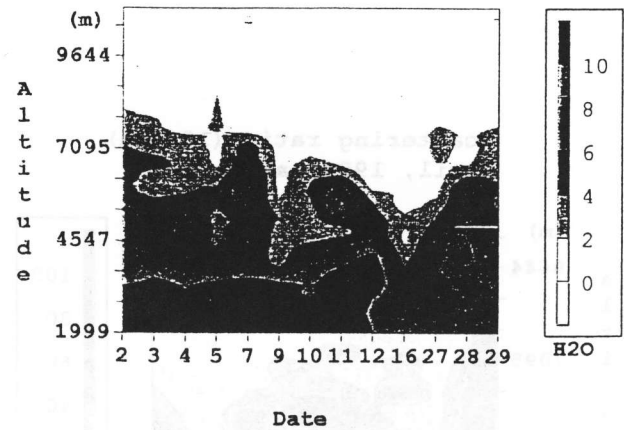
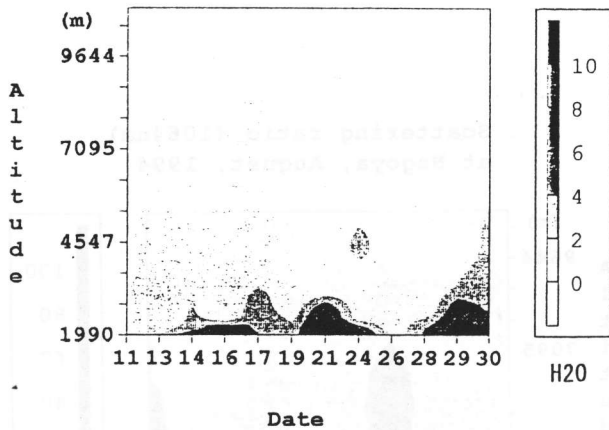


Depolarization ratio  
at Nagoya, August 1995.



Water vapor mixing ratio (g/Kg)  
April, 1994. at Nagoya

Water vapor mixing ratio (g/Kg)  
August, 1994. at Nagoya



# 3-D distribution of atmospheric particles

Optical properties

Chemical Composition

Surface Structure  
(Shape, Surface Area)

Radiation  
放射

Geochemical  
Cycle of N,  
S, ...  
地球化学